Overview of KSTAR Initial Operation

M. Kwon 1)
on behalf of the KSTAR Team

1)National Fusion Research Institute, Daejeon, KOREA

e-mail contact of main author: kwonm@nfri.re.kr

1. Introduction

As was reported in the previous IAEA meeting, KSTAR finished successfully the first plasma generation in the middle of 2008, and entered the initial operation phase from 2009 [1]. In this paper, we will present a detailed report of the major researches and upgrade results of the initial operation for last two campaigns.

The KSTAR device is a medium-size, D-shaped tokamak with the major machine parameters of R=1.8m, a=0.5m, B=3.5T, I_p=2MA, κ_x=2.0, and δ_x=0.8. Its main research goal is to demonstrate the steady-state operation in the high-performance, advanced tokamak (AT) modes, and KSTAR adopted several advanced features to support this goal, which include fully superconducting magnet system, flexible heating and CD systems with long-pulse operation capability, strong plasma shaping capability with a conducting wall close to plasmas, and advanced diagnostics and control systems. With these features, KSTAR is expected to play a significant role as a new device capable to address many scientific and technical issues, critical for the development of steady-state, high-performance operation scenarios related to ITER and advanced DEMO reactor.

From the core physics point of view, "steady state operation" is defined as "a discharge duration longer than several plasma current diffusion time τ_R (10^{-1} to few tens of seconds depending on the devices) to reach constant loop voltage condition" [2]. Comparing τ_R with typical characteristic time of technological aspects of tokamak operations, necessity of the long-pulse operation is shown clearly: ~10 sec to the thermal equilibrium of PFCs, ~100 sec to the wall saturation time, ~ 10^6 sec for the lifetime of plasma facing components. This simple comparison gives issues that should be considered for steady-state operation: the sustainment of magnetic configuration by superconducting coils and non-inductive current drive systems, the operation and control of kinetic configuration including pressure, rotation and particle content, and the reliable operation of super-conducting magnets, heating and current drive systems, plasma facing components and diagnostics. Describing briefly some of such issues and the possible KSTAR role, KSTAR is expected to play key role as a test-bed of ITER superconducting magnet system, which is made by the same material, Nb_3Sn, as for KSTAR. KSTAR will provide rich experiences of the operation characteristics, including the AC-loss, of the PF coil system and the He refrigerator and of the operation skills to avoid the quench with maximum efficiency. The optimum scenario for a full non-inductive current drive will be also explored in KSTAR, using its flexible heating and CD systems which include NBI, ICRH/FWCD, LHCD, and ECH/ECCD. Particularly, we will try to maximize the bootstrap current fraction with a good alignment, which is a critical element required to achieve the AT modes. A significant effort will be also put on the development of an advanced divertor system, which can withstand the long-pulse operation in the high power-density condition, expected in the AT modes. The control of particle and impurity is also an important issue for the steady-state operation, and an intensive study will be performed on the subjects, such as the wall recycling, saturation, retention, erosion, and dust particle. To achieve the disruption-free long-pulse operation of high-beta plasma, it is also critical to develop a robust active control capability of various MHD instabilities, which include the locked-mode, NTM, ELM, and RWM. We will try to develop this capability utilizing the in-vessel control coil, pellet pace-making system and other actuators such as ECH in KSTAR. Finally, it is natural to plan to make a substantial effort for the control of plasma transport and profiles, such as the plasma current, density, temperature profiles and the local transport barriers. Utilizing the advanced diagnostics and control systems, and also the long-pulse operation capability, the plasma profile will be detected and adjusted in real time for the realization of optimum target profiles, required for the AT mode with a high-confinement, high-beta, and high bootstrap current fraction.

In order to address the research issues and to achieve the research goal described above, it is now planned that KSTAR will be gradually upgraded in operations and the ancillary systems such as heating and CD systems. It should be noted that our basic strategy is to develop the steady-state, high-performance operation scenarios in the relatively low or medium power-density regime for the first-half period till 2018,

aiming at supporting more ITER-relevant researches, and then upgrade the scenarios to the high power-density regime to support the advanced DEMO-relevant research in later part of operation period.

The cool-down for the 3rdcampaign was started from July 2010 and plasma experiments are now under way. The main research goal of the 3rd campaign is to achieve the D-shape plasma with the position and shape control using the in-vessel control coil (IVCC) and PF coils, and then perform some physics study of Ohmic and L-mode plasmas with the initial heating power from NBI, ICRH, and ECH system. Some initial results of the 3rd campaign experiments will be reported at the conference.

2. Device Updates

After completion of the construction in the middle of 2007, KSTAR succeeded in production of the first plasma in 2008, and in control of circular plasmas in 2009 campaign. However, absence of few important systems imposed a major limit on the studies for the steady-state operations.

For the preparation of the 3rd campaign of KSTAR, many in-vessel components such as inboard limiter, divertor, passive stabilizer, in-vessel control coils (IVCC), in-vessel cryo-pump (IVCP), and various kinds of diagnostic systems have been newly installed for up to 20 sec long pulse operation. Extensive baking and cooling of the components are required for the steady-state operations with desired density control. Vacuum vessel and pumping duct were baked at a temperature of 130 ℃, and PFCs to 225 ℃ (capable up to 350 ℃) by hot nitrogen gas (GN_2). Boronization is a good wall conditioning method to reduce oxygen and metallic impurities before running long pulse discharges. For safety reason, boronization in KSTAR uses carborane solid powder ($C_2B_{10}H_{12}$) [3]. Boronization is successfully performed in the 2nd campaign, and the water and oxygen impurities were effectively removed. The Glow Discharge Cleaning (GDC) is also a good method to control wall pumping. For a machine equipped with superconducting coils, ICRH or ECRH wall conditioning (ICWC or ECWC) would be another choice. Wall conditioning including in-between ICWC is performed regularly to have a better wall condition and density control [4]. Figure 1 shows the current machine status of KSTAR, actively preparing for its long pulse mission step by step to become one of promising candidates for ITER pilot devices.

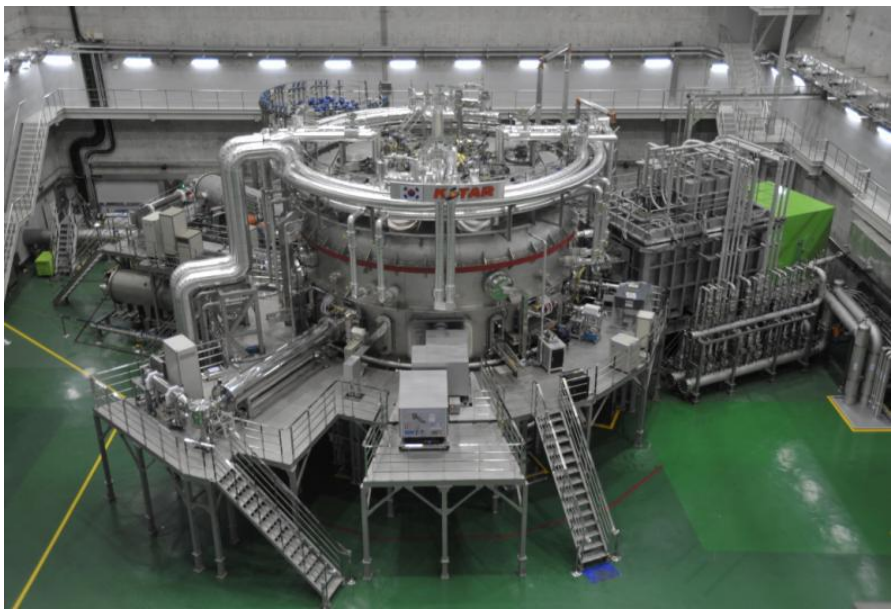

Fig. 1 Current status of KSTAR under the 3rd experimental campaign.

Since deficiency of key H&CD devices such as neutral beam injection (NBI) system, electron cyclotron current drive (ECCD) system, and lower hybrid current drive system (LHCD) may decisively impact not only on the 2010 campaign but also on the forthcoming steady-state operation experiments, it should not be underestimated the importance of the H&CD system development.

The AC-loss of super-conducting magnet systems is an important issue for the steady-state operation of tokamak such as KSTAR and ITER. In KSTAR, the AC-loss causes the temperature increase of the liquid-He by few degrees which could endanger a safe operation limit of the poloidal field magnets. Characteristics of AC magnets in KSTAR have been measured and symptoms leading the liquid-He temperature close to the

quench limit have been observed. Remedies have been sought and tested including the flow rate increase and the delay of current-ramp rate [5].

2.1 Plasma Facing Components

As shown in Fig. 2, the KSTAR plasma facing components (PFC) consists of inboard limiter, divertor, passive stabilizer, poloidal limiter, and NB protection armor. Heat-sink plate of the inboard limiter has a toroidally continuous cylinder-shape, which are made of stainless steel (SS316LN) with internal cooling channels for active water cooling and baking. The plate is installed on the straight section of the vacuum vessel, and is covered by graphite tiles that are simply mounted on the plate by bolts. Total 16 sub-segments of the inboard limiter is covered by graphite tiles, however, before the long-pulse operation starts, four sub-segments will be replaced with carbon fiber composite (CFC) tiles, on which energetic neutral beam strikes and strong heat influx takes place.

The divertor system consists of inboard, central and outboard parts. Each part contains 8 heat-sink plates that locate in upper and lower side of the vacuum vessel with up-down symmetry for double-null (DN) operation. Entire area of the heat-sink plates is covered with graphite tiles but eventually with CFC tiles by bolts to withstand high temperature (maximum 1,200 °C) at a striking point for the case of maximum heat influx of 4.3 MW/m^2.

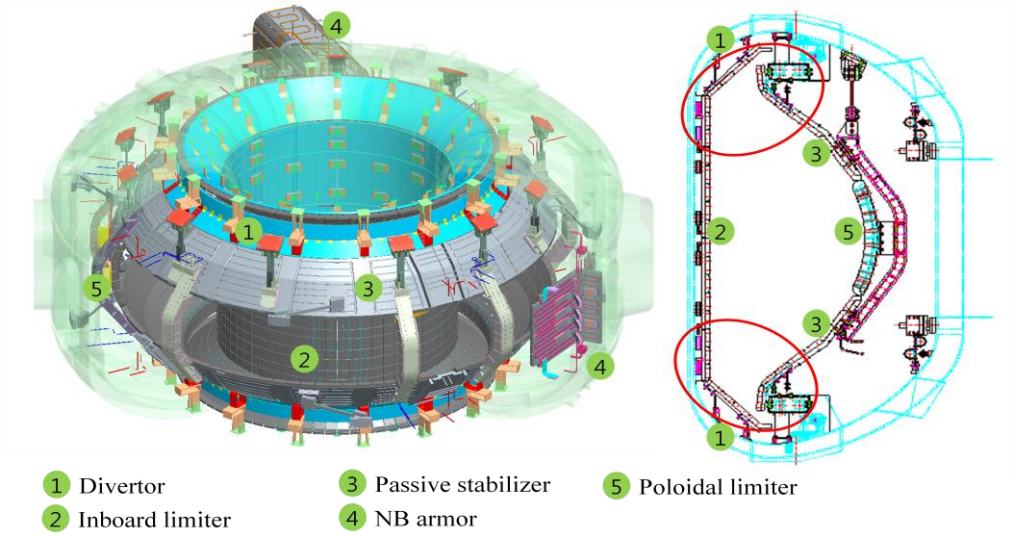

Fig. 2 Configuration of KSTAR In-Vessel Components

The passive stabilizer will play roles both on plasma position control and on suppressions of MHD instabilities through various combinations with active control coils. Two toroidal ring-shaped copper plates made of CuCrZr alloy have up-down symmetry. Each plate is electrically segmented into four quadrants, and a quadrant is electrically connected to an adjacent quadrant by “gap resistors” to adjust total resistance of the passive plate in toroidal direction. The design was optimized through a trade-off study between the controllability of n=1 RWM mode and the controllability of vertical instability by the IVCC. For improving the penetration of magnetic field induced by the IVCC, the number of gaps increased to four but this change did not degrade much the suppression capability of n=1 RWM [6]. The poloidal limiter comprises three D-shaped strings to protect launchers of the ICRF and the LHCD. Because the KSTAR NBI system is composed of two beam lines, the NB protection armor system also comprises two sets of actively cooled CFC tiles.

2.2 In-Vessel Control Coil (IVCC)

The IVCC system was developed to take advantages of active control of the plasma position, the field error correction (FEC), and the resistive wall mode (RWM) [7, 8]. More recently, the IVCC is expected to be effectively utilized in suppression of edge localized mode (ELM) [6,9]. This important system adopted a unique concept of segmented coil assembly, having 16 segments and their support structures [10]. Each segment contains eight water-cooled normal copper coils that are partially connected to an adjacent segment in series to form four circular coils for position control as shown in Fig. 3, while remaining copper

conductors are connected to the vertically neighboring segment to form twelve "picture-framed" coils for the FEC and RWM control. The eight copper coils in a segment are finally encapsulated by 3 mm thick of jacket made of stainless steel (SS316LN).

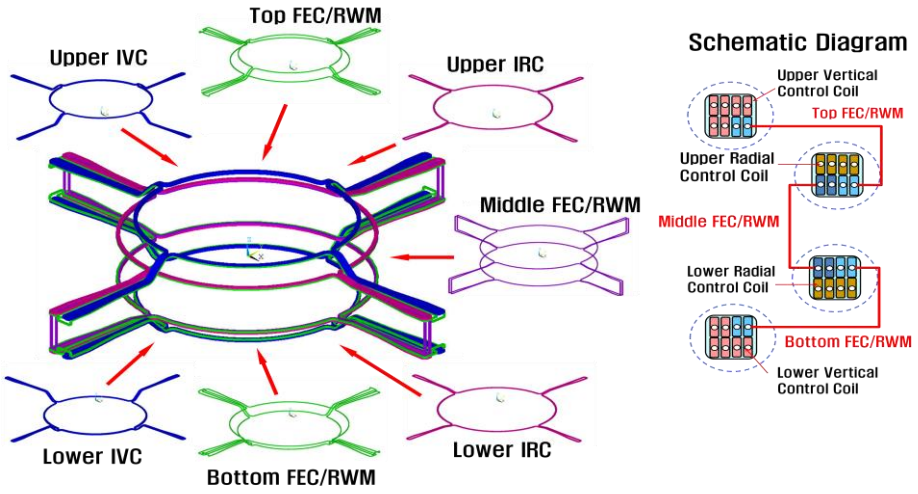

Fig. 3 Electrical connection scheme of the IVCC

2.3 Neutral Beam Injection System

A bucket type positive ion source, which has been developed by Korea Atomic Energy Research Institute (KAERI) from early stage of the KSTAR construction phase, has demonstrated 55 A of hydrogen ion beam at 100 keV with 2 s in the beam pulse [11]. The source also achieved 300 s in the beam pulse length with 33 A at 90 keV for long-pulsed operation. More recently, the source was substantially modified by replacing the source chamber to enhance the arc efficiency.

Procedure of the ion source conditioning was started from the filament heating, then moved to the high voltage insulation test at the grid. Then the high voltage was applied to the accelerating grid up to 82 kV and the decelerating grid up to -2 kV with the maximum pulse duration of 30 s. Figure 4 shows the beam extraction results. The optimum arc power is investigated to get the beam perveance close to the designed value of 1.2 μ-perveance as the accelerating beam voltage increases. The waveforms of voltage and current at the filament and arc power supplies, the accelerating power supply, and the decelerating power supply are also shown in Fig. 4.

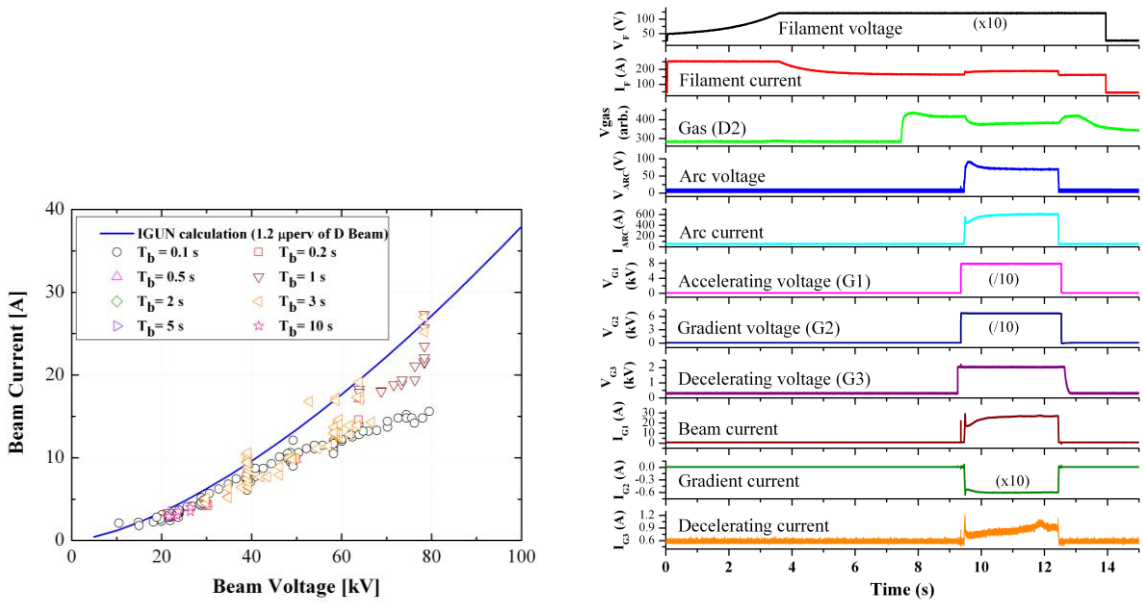

FIG. 4. (Left) The beam perveance data and (right) the waveforms of the 3-s beam extraction with the beam energy of 80 keV and the beam current of 27 A. The filament voltage and current are those of the filament no. 3.

The 6.5 MJ deuterium beam extraction at the 80 kV and 27 A is achieved using the calorimeter beam dump. As seen in Fig. 4, the beam is extracted by the arc discharge. The beam current rises very slowly to

the flat level with a slope of about 58 A/s at the initial current ramping region. But, it takes about 2 s for the current reaches to the flat level. The pre-arc discharge without the beam extraction is attempted for the prompt current rise within 50 ms. This method would be useful for the beam injection to the torus with short pulse duration.

2.4 ECH/ECCD System

Success in the ECH-assisted startup using 2nd harmonic [12] EC wave is expected to provide lots of crucial techniques for reliable startup with relatively low loop voltage (~ 3 V) in superconducting tokamak devices. The KSTAR ECH-assisted startup system originally utilized a 84 GHz gyrotron with a capability of 500 kW and 2 s pulse length. As a backup, another system was prepared with a 110 GHz gyrotron, which has specification of 800 kW for 2 s pulse length and 500 kW for 5 s pulse length and diode-gun type with no depressed collector, loaned from General Atomics (GA). The 110 GHz ECH system was used for the second harmonic EC resonance at the toroidal magnetic field of 2 T.

In addition to the ECH-assisted startup system, a 1 MW, long-pulse, 170 GHz ECCD system is another important one for Neo-classical Tearing Mode (NTM) control, saw-teeth mode control as well as electron heating and current drive. The 170 GHz gyrotron which has been developed by JAEA (Japan Atomic Energy Agency) for pre-prototype of ITER ECH will be loaned early 2011. Test results on the gyrotron they achieved are quite satisfactory to the KSTAR requirements.

2.6 LHCD System

A 5 GHz LHCD system that uses same frequency for ITER system [13] will play key roles in providing plasma current and controlling its profile. To investigate the issues of steady-state operations, the initial LHCD system is scheduled to be installed in 2011 using the prototype of 5 GHz, 500 kW CW klystron and the un-cooled, fully active, phased-array waveguide launcher.

The prototype klystron fabricated by Toshiba in Japan, was successfully tested at KSTAR site. The power output was achieved more than 460 kW for 20-s, and 300 kW for 800-s. The launcher of the initial LHCD system will be composed of 2 arrays, each with 8 waveguides in column with consideration of the power upgrade to 1 MW [14]. For injection of the 5GHz LH wave into the plasma, an LH launcher was designed based on the 4-way splitter without active water cooling.

3. Recent Experimental Results

3.1 Plasma start-up and control

The start-up of the KSTAR device differs from typical tokamak start-up in two aspects. First of all, the KSTAR device requires a Blip Resistor Insertion System (BRIS) to produce sufficient change of poloidal field (PF) coil current during the initial stage of discharge due to limited voltage capability of PF power supplies. In order to use the BRIS, outer PF coils also need to be charged even though magnetic field generated by those coils degrades initial field null quality [15]. This complicates the start-up of the KSTAR device due to short connection length of charged particles to the wall.

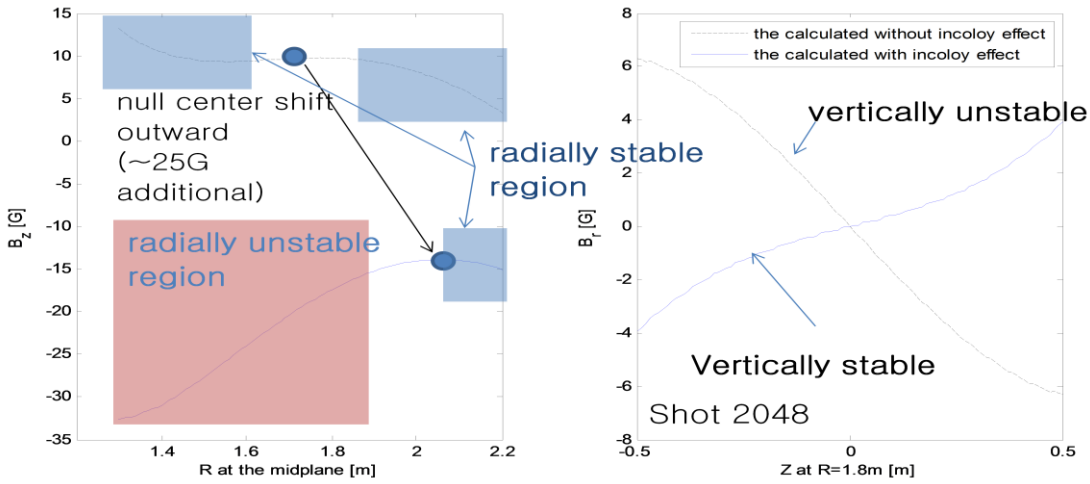

Fig 5. The effect of Incoloy on the field-null. The sign of B_z & B_r near field-null center changed from the influence of Incoloy.

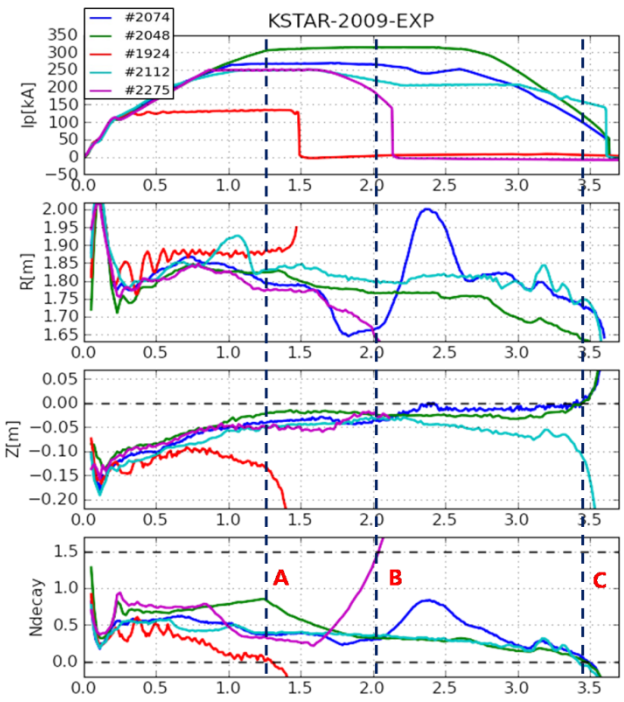

Fig. 6 Basic stability analysis of KSTAR 2009 plasmas. According to the decay index of magnetic field, it clearly shows that shot 2275 was terminated by RDE and the others by VDE.

The other unconventional aspect of KSTAR start-up originates from the ferromagnetic material, Incoloy 908 used in the PF and toroidal field (TF) coils. The impact of this was quite serious during the start-up phase. Roughly speaking, Incoloy is generating approximately -20 G vertical field at the field-null center and its inclusion in the startup scenario development is important to overall startup success in KSTAR [16,17]. Based on the FEM analysis of Incoloy, it was determined that the effect of Incoloy on the startup was not trivial. Although the effect of Incoloy on the vertical field profile is roughly constant and it does not change the vertical profile much, its effect on the radial profile is more complicated. As shown in Fig. 5, due to a strong impact from the Incoloy in the central solenoids, the radial profile is completely different from the case without Incoloy. Consequently, not only does it degrade the initial field-null quality but the position stability of the initial plasma column can be affected by the modified field index from Incoloy and therefore a simple offset correction for Incoloy is just partially effective. The field decay index, $n=-(dB_R/dz)/(B_z/R)$, has a negative value for vertically unstable plasma and a positive value larger than 1.5 for radially unstable plasma. Therefore positional stable plasma should have a positive value ranged from zero to 1.5. Figure 6 shows results of basic stability analysis [18] for several representative shots in KSTAR 2009 campaign. The field decay index was calculated at the effective center of plasma column with reconstructed magnetic fields excluding plasma contributions. As shown in the figure, the field decay index of the shot 2275 exceeded 1.5 that. Similarly other shots such as 1924, 2048, 2074, and 2112 show that the field decay index became negative around the time points of A and C, so that those shots were terminated by VDE (Vertical Displacement Event). The plasma control system (PCS) for KSTAR has been developed based on the DIII-D system for ensuring the positional stability after start-up phase and for shape control by adopting the real-time EFIT.

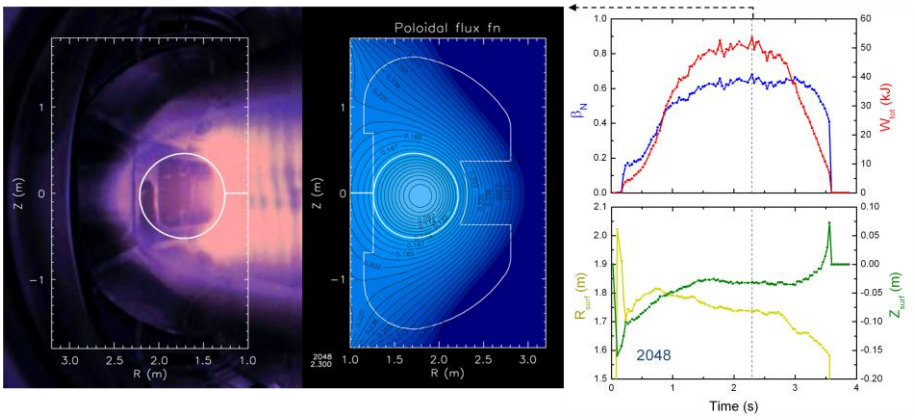

Fig. 7 a) Fast frame camera image and reconstructed equilibrium flux surfaces at t = 2.3 sec for shot 2048. b) Evolution of reconstructed normalized beta and toroidal plasma stored energy and c) plasma radial and vertical position.

The equilibrium reconstruction is routinely done with EFIT as shown in Fig. 7 and it also showed the evolution of the stored energy and the beta value [6]. In Fig. 7, the plasma was shifted downward during the position control and this downshift of plasma column during the ramp-up phase suggests existence of certain level of the radial magnetic field (Br) at the midplane so that the potential sources of Br are also investigated. It turns out that the eddy current flowing in the up-down asymmetric cryostat structure may provide the required Br for the downshift. When cryostat is included in the FEM model, the simulated voltage is in better

agreement with the measured one by flux loops and it suggests that the effect of cryostat is not trivial and its effect is larger on the outer flux loops installed in an up-down symmetrical way. However, it may be easily compensated with slightly up-down asymmetric charging of outer PF coils or in-vessel control coils.

Systematic efforts are being conducted to establish robust start-up scenarios with compensation of the aforementioned ferromagnetic materials and the asymmetric eddy current effect. When incoloy effect is added, field structure in Fig. 8a) is transformed to field null structure as shown in Fig. 8b). Indeed, charged particles feel the field structure depicted in Fig. 8b) rather than in Fig. 8a). After the formation of plasma current channel, vertical magnetic field needs to increase along with plasma current ramp-rate to satisfy a toroidal equilibrium. Due to the incoloy effect, the actual value is almost 35 gauss lower than the value without the incoloy effect. It is noteworthy that gradual transition from initial field null state to favorable field curvature is essential. Those experiences with the magnetic materials can be applicable to the ITER startup since there will be a considerable amount of ferritic materials around the main tokamak structure in ITER [19].

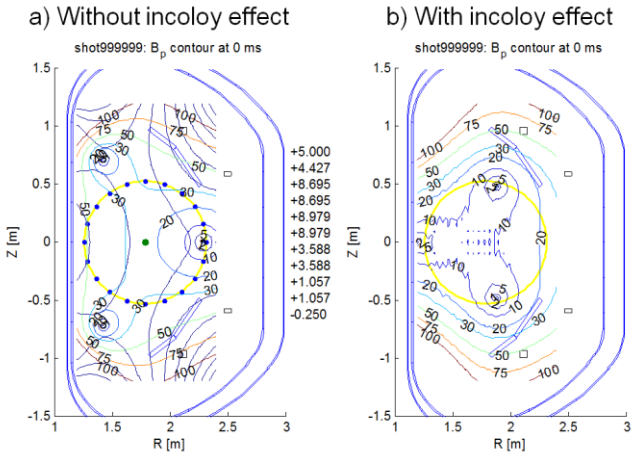

Fig. 8 Initial magnetization state of ECH-assisted start-up for the 2010 KSTAR campaign. Field null structure is formed when incoloy effect is included.

3.2 Second harmonic ECH pre-ionization

The second harmonic electron cyclotron heating (ECH)-assisted startup has been established to provide the reliable plasma startup with low toroidal loop voltage in KSTAR. For 2008 first plasma campaign, the KSTAR is operated with toroidal magnetic field of 1.5 T at the major radius of 1.7 m which corresponds to the second harmonic resonant field with 84 GHz EC wave. For 2009 plasma campaign, KSTAR is operated with TF field of 2 T at the major radius of 1.8 m which corresponds to the second harmonic resonant field with 110 GHz EC wave.

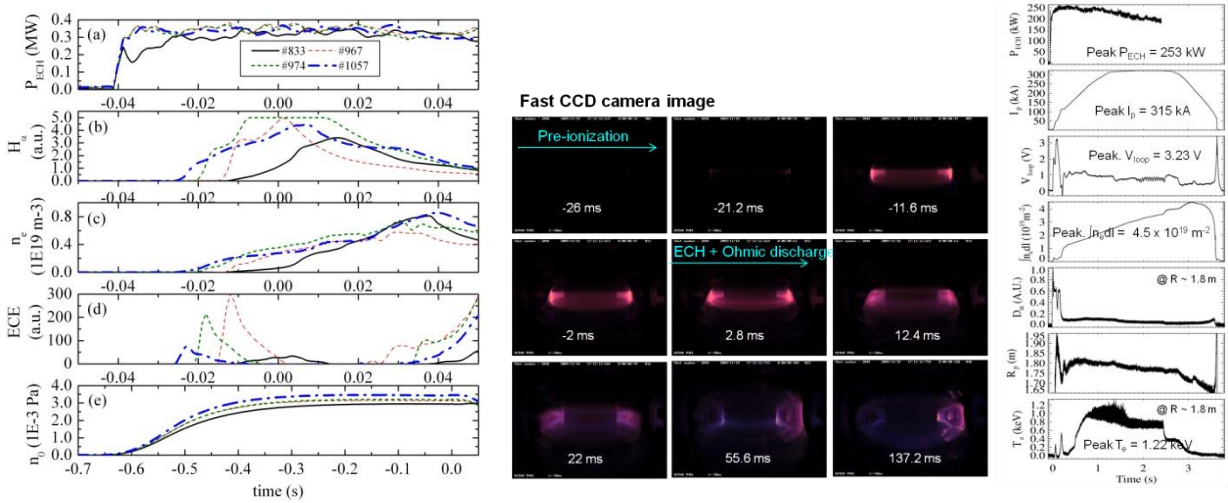

FIG. 9 (Left) The typical 84 GHz second harmonic ECH pre-ionization experimental results for different beam launching angles and (right) the 110 GHz second harmonic ECH-assisted startup in 2009 campaign with the snapshots of the CCD-pictured plasmas.

The experimental results during KSTAR 2008 and 2009 campaigns showed the feasibility of the second harmonic 84 and 110 GHz ECH-assisted startup with the low loop voltage ranged from 2 V (0.24 Vm-1) to 3 V (0.36 Vm-1) [12]. The application of the EC beam before the onset of the inductive toroidal electric field

provided a localized plasma confined by the poloidal magnetic field null (FN) structure which was obtained by the initial magnetization in 7 pairs of the poloidal field coils. It also allowed the burn-through and sustained the plasma during the current ramp-up. The optimized condition of ECH pre-ionization was investigated with parameter scans of hydrogen and deuterium pre-fill gas pressure, resonance position, polarization, and vertical magnetic field without Ohmic discharge. The pre-ionization was very efficient at the higher pre-fill gas pressure and the oblique beam injection crossing the resonance position. The oblique injection angle of 15 degrees was the best condition to provide the reliable ECH-assisted startup. The pre-ionization was delayed at the low pre-fill pressure, the inboard resonance position, O-mode injection, and the higher B_z at the FN center, as evidenced by the D_α emission and the central ECE signal. Figure 9 shows the 84 GHz and 110 GHz ECH-assisted startup using the second harmonic pre-ionization in 2008 campaign and 2009 campaign, respectively.

3.3 Particle control

A good initial vacuum and wall conditioning procedure is essential to obtain high-quality wall condition for plasma experiments. Various kinds of wall conditioning techniques have been utilized to remove impurities from the surface of plasma facing components including H_2O, carbon and oxygen compounds [20]. Wall conditioning in KSTAR consists of baking, glow discharge cleaning (GDC), ICRH Wall Conditioning (ICWC), and boronization (Bz)

The operational windows for GDC have been scanned and the optimization is underway. In a He GDC, a particle removal rate of ~10^{18}-10^{19} particle/sec is obtained while that of ICWC is ~10^{17}-10^{18} particle/sec. $H_{implanted}/D_{pumped}$ during the ICWC is about 5-15. Pulsed operation seems more effective than CW. From the observation by in-vessel TV system, it seems that the cleaning is effective at low field side out-board. Also, the homogeneity of the plasma has to be improved by applying external poloidal magnetic fields. The ICWC results are consistent with that from other machines.

Various ICWC parameters have been scanned: Pressure (He/H_2 mixture rate) and power coupling (CW, duty cycle). The response of the wall to the RF plasma is measured by RGA signals and emission spectroscopy. On the other hand, ICWC in between shots has been performed regularly during the campaign. Note that, because the TF field of the plasma shots was 2 T, no resonance layer was present in this case. Figure 10a) shows numbers of molecules for masses M_2 and M_3 depending on the H_2 mixture rate. By using a night D_2 GDC, The wall was saturated by ~10^{24} D atoms (similar to TS [21]). As He/H_2 ICWC is performed, the isotope exchange has occurred. The retention of H increases, as M_3 release increases. As the wall is saturated by H at 80 sccm, the H retention starts to decrease, thus production of HD decreases, too. The number of $H_{implanted}$ is an order of ~10^{21}, while that of D_{pumped} is ~10^{20} with a ratio of $H_{implanted}/D_{pumped}$ ~ 5-15. The H retention rate is of the order of ~10^{19} H/sec. Similarly, Tore Supra has reported the H retention rate of about 3×10^{19} H/sec with no sign of saturation, while in TEXTOR about 1-2×10^{20} H/sec with a slight sign of saturation [22]. Note that, we cannot separate D_2 and He by RGA. Nevertheless, the ICWC results from Tore Supra have shown that the D_2 partial pressure during the ICWC is small compared with that of HD (~10%) [21]. Thus, the estimated amount of D_{pumped} in the measurements would have about 10% error bar.

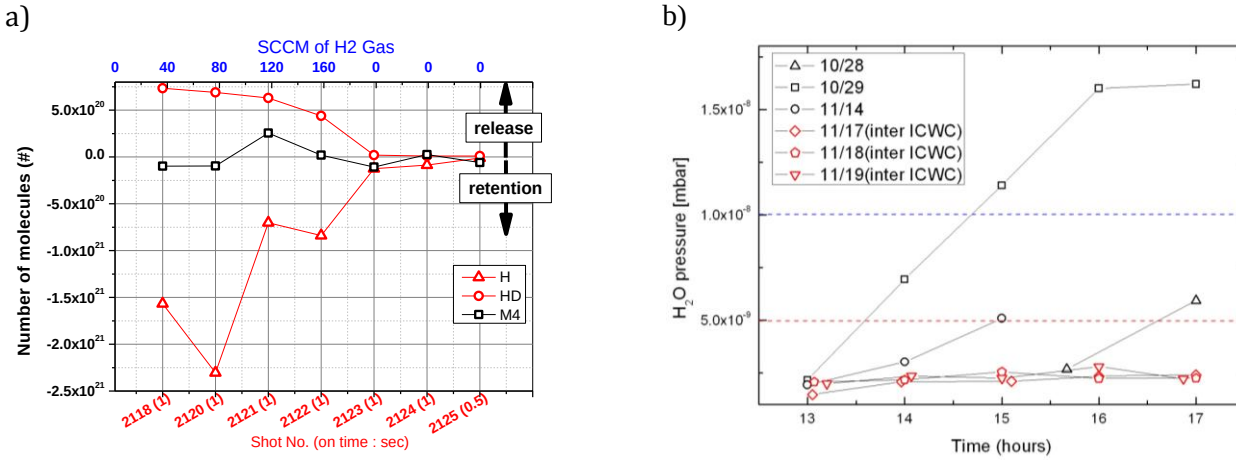

Fig. 10 a) Numbers of molecules of M_2 and M_3 depending on H_2 mixture rate. b) Water removal by inter-shot ICWC during the campaign.

The H removal rate of He ICWC (~10^{18} H/sec) is about 5-10 % of that in GDC. The HT-7 and EAST showed that absolute H removal rate of 1-4×10^{19} H/sec [22].

Figure 10b) shows an example of the water removal by inter-shot ICWC. During the 2nd campaign, water was the dominant impurity through the campaign with an average percentage of about 7 %. Without Inter shot ICWC, the water pressure increases rapidly in several hours up to 1.5×10^{-8} mbar. The increase of the water pressure is effectively suppressed by inter-ICWC.

First boronization in KSTAR was successfully performed by using carborane vapor. Water and oxygen level in vacuum vessel have been reduced significantly. However, additional H atoms dissociated from carborane mother molecule world be a small problem for the density control during following shots. Boron containing thin film deposited by boronization is a hard diamond-like film with small amount of boron components with a density of 2.0-2.2 g/cm^3, H/H+C ratio of 25-30 %.

3.4 Dust characterization

Dusts created by flaking and brittle destruction have non-spherical shape while that created by arcing and volume polymerization have spherical shape: Spherical particles are spontaneously formed when critical density of molecules of materials exists in unit volume of plasma, so called "supersaturated vapor condensation". Although its creation mechanism and birth place are still under discussion, the presence of hydrogenated carbon (a-C:H) nano-particles of size smaller than 0.1 μm in diameter with a well defined Gaussian distribution within a certain full-width half maximum (FWHM) is identified in many machines equipped with graphite plasma facing components. This is a clear evidence of plasma volume polymerization [23,24] in fusion devices. This reveals that a parameter window for nano-particle formation exists, even in fusion plasmas, with sufficient amount of hydrocarbons exceeding the critical density for the initiation of the process.

Another striking fact observed in KSTAR is the incorporation of hydrocarbon nano-particles into layers at vertical ports. It is found that a-C:H nano-particles have onion-like internal shell structures. Inner shell (r<50 nm) has small amount of hydrogen (H/C~0.4) due to high temperature during the growth of nano-particles, but outer shell (r>50 nm) has H/C ratio larger than 1. Hard a-C:H films have very strong internal stresses so that they pile off from the surface of the substrate where they are deposited when their thickness exceeds the limit (usually 0.5-1 μm). In order to increase the thickness of an a-C:H thin film over the limit, hydrogen has to be removed or small nano-particles has to be incorporated. This clearly reveals two very important facts for ITER operation and safety. First of all, these nano-particles would have no effect on the operation because they are tightly bonded to the layers. Recent DIII-D observation during the ITPA urgent task “injection of pre-calibrated dust” indicates that dusts can be mobilized before the plasma start-up and they disturb the start-up.

On the other hand, although ITER uses full tungsten divertor during D-T phase, carbon will be present in the machine due to the co-deposited layers at shadow regions. There is always possibility that a-C:H nano-particles are formed during ITER operation. As soon as ITER uses tritium, the T retention in the a-C:H nano-particles created in the D-T phase can be significant. Recent calculation of T retention in hydrocarbon nano-particles in ITER during a MARFE in D-T phase with 1% of carbon impurity density is about 3.6 g [25]. Therefore, once these nano-particles are incorporated into layers, layers can grow easily up to several tens to hundreds μm due to stress relaxation by nano-particles, and tritium incorporated into nano-particles cannot be collected unless entire layers are removed.

3.5 Analysis and prediction

Here, we introduce briefly some theoretical and simulation work performed for the experimental data analysis and operation scenario modeling of KSTAR over the last two years. Firstly, in relation to the ECH-assisted start-up, an analytic study has been performed of the electron cyclotron resonance heating process in the 1st and 2nd harmonic resonance cases [26,27]. A net energy gain when particles go through a resonance zone was calculated using a collision-less nonlinear cyclotron heating model with a realistic wave beam profile. It is found that the axis and frequency of nonlinear energy-oscillation are about one order higher so that electrons can gain the energy up to several hundred eV in the 1st harmonic resonance case, while only up to ~10 eV in the 2nd harmonic one. Thus, ECH can heat up low-energy electrons of room temperature order to several hundred eV rapidly with the first harmonic resonance, while it takes a longer time for the 2nd harmonic case. This theoretical model thus provides a qualitative explanation for the delay of pre-ionization time observed in the 2nd harmonic ECH experiment.

A new theoretical model has been also developed to explain the observed plasma current during the ECH pre-ionization experiment, where a few hundreds of Ampere was repeatedly measured even when the ECH

beam was launched vertically to the toroidal magnetic field with no preferable toroidal direction [28]. Noting that the only factor breaking the toroidal symmetry is a tiny vertical magnetic field within the field null region, and the average life time becomes different between the electrons flying to clockwise or counter-clockwise when the vertical motion due to this small field combines with the grad-B drift, an analytic calculation was done to obtain a finite ECH driven electron current for a given density, temperature, and vertical magnetic field. It is found that the calculated current is well within the order of the experimental observation, thus providing another explanation different from the previous model by Forest et.al [29], where the ECH driven current was explained by the Pfirsh-Schluter, bootstrap, and precession-drift current models.

In relation to the KSTAR divertor experiment to be performed soon, a two-dimensional simulation study has been also made of the transport of divertor plasmas in the KSTAR model by using the B2.5 code [30]. Maximal divertor heat fluxes were evaluated in the sheath-limited regime at various powers, and the effect of C impurities on the divertor heat flux was investigated. It is shown that the C impurities change the intensive radiation position from the outer SOL region near the divertor to a private region near the X-point, and the radiation near the X-point gives rise to effective removal of the peak heat flux. The change in the intensive radiation position appears to induce an increase of the heat influx to the private region from the SOL across the separatrix, resulting in a significant reduction of the divertor heat flux near the striking point.

Finally, a detailed analysis has been done for the ideal MHD stability limit of the KSTAR target AT modes [31]. For a set of model equilibria with the reverse-shear q-profile the stability boundary of the low-n external kink modes was calculated using the two codes of DCON and GATO. It is found that the dependence of β_N limit on the toroidal mode number n changes significantly with the pressure profile. In the relatively peaked profile [Fig. 11(a)] the β_N limit increases with n, so that the possible maximum β_N is almost decided by the n=1 mode. Meanwhile, in the cases with broader pressure profile [Figs. 11(b) and (c)], the β_N limit decreases with n, making the maximum β_N determined by higher n modes (n=3, here). With this change in the mode number of the most unstable mode, the maximum β_N value decreases substantially as the pressure profile becomes broader, as shown in Fig. 10.

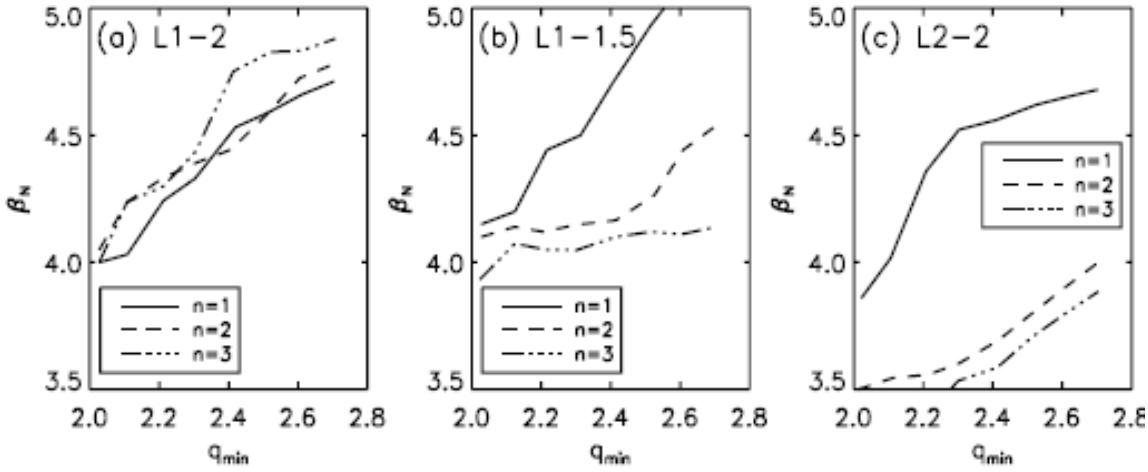

Fig.11 β_N limits of the n=1-3 modes as functions of q_{min} for three different pressure profiles.

4. Summary and Near-term Plan

In this work we have presented a detailed report on the initial results of machine upgrade and experimental research in KSTAR, which entered the experimental operation phase from 2009. As was shown in Ref. [32], with the planned heating and CD systems in couple of years, it was predicted that most of the important features of the steady-state, AT mode of operation can be achieved in KSTAR; fully non-inductive, high performance, high confinement, high bootstrap current fraction and keeping these features for longer pulse duration. Other features which cannot be considered for the simulation work, such as the optimized operation of the liquid-He facility, better particle control, efficient power exhaust and active suppression of MHD modes with reliable actuators and control system should also be prepared and practiced reliably.

Summarizing some of the major results, firstly for the machine upgrade, all of the plasma facing components (PFCs), which include inboard limiter, divertor, passive stabilizer, have been installed inside the vacuum vessel. The sixteen segmented in-vessel control coils were also installed between the PFCs and the vacuum vessel. In addition, the first NBI system (NBI-1), designed to deliver 8 MW deuterium neutral

beams into the KSTAR plasmas with three ion sources, was installed and tested. Besides, substantial upgrades have been made in diagnostics, control, power supply, and other heating/CD systems.

For the experimental research, after the 1st plasma experiment in 2008 the 2nd campaign was carried out in 2009 and the 3rd one is now under way. Here, summarizing some of the major results from the 1st and 2nd campaigns, Ohmic plasma current was ramped-up over 300 kA with the pulse length of more than 2 seconds. Toroidal field was increased up to 3.6 T, exceeding the design limit of 3.5 T. A substantial progress has been made in resolving the start-up issues, particularly related to the stray field by the Incoloy 908 magnetic material in superconducting coils and the eddy current by the up-down asymmetric cryostat structure. The ECH-assisted start-up scenarios with the relatively low loop-voltage of about 2V were established well with the second harmonic pre-ionization using 84 GHz/350kW and 110 GHz/250 kW gyrotrons at the toroidal field of 1.5T and 2 T, respectively. Several wall-conditioning methods, such as GDC, ICWC, boronization, and baking were tested and now being routinely utilized. The study of dust particles was also started using dust collectors and coupons.

Finally, we here introduce briefly the near-term KSTAR operation plan for 2011-2012. As summarized in Table 1, for the 2011 campaign a main target goal is to get the H-mode plasma reliably. The heating power will be upgraded to about 5 MW, which is estimated to be well above the H-mode threshold value. Diagnostics will be also upgraded for the measurement of plasma properties near edge and divertor region. The initial study will be then performed of the basic characteristics and physics of H-mode plasma, such as the energy confinement time, L-H transition, pedestal, plasma rotation, and ELM control. During this year the plasma current will be also increased up to 1MA with the pulse length of about 10 sec, and a more detailed physics studies will be made of MHD instability, plasma heating, and plasma wall interaction issues. Besides, initial study will be done on the single-null (SN) plasma, and 5 GHz LHCD system will be commissioned with the initial power of 0.3 MW.

For the 2012 campaign, plasma current will be increased further, targeting to reach up to 2 MA with the pulse length of 20 sec in pure ohmic mode. The research of H-mode plasma will be continued focusing more on the detailed physics study in high toroidal magnetic field up to 3.5 T. For this, diagnostic system will be upgraded substantially, particularly to implement the turbulence measurement systems, such as MIR and BES. The active control of ELM as well as field error will be also possible through the upgrade of IVCC power supply system. The high-field-side pellet injection system will be also available for the study of particle transport and density profile control. A study of current drive experiment will be also performed of the current profile control using the NBCD, ECCD and LHCD system, targeting for full non-inductive, steady-state operation which will be the main research area for the next operation period of KSTAR.

Table 1. Schedule of the KSTAR operation and system upgrade for the initial 5 years

Campaign	2008	2009	2010	2011	2012
Operation Time	'08. 3 ~'08. 8	'09. 8 ~'09.12	'10.6 ~'10. 12	'11. 4 ~'11. 9	'12. 3 ~'12. 8
Experimental goals	• First plasma startup • 2nd Harmonic ECH pre-ionization	• Startup stabilization • ECH pre-ionization • ICRF wall conditioning	• Shape control • L-mode • MHD study • Wall conditioning	• H-mode • MHD • Disruption • Wall interaction	• Profile control • ITER shape • ELM & disruption
Operation Parameters	• B_T ~ 1.5 T • I_P > 0.1 MA • t_P > 0.1 s • Te ~ 0.3 keV • Shape ~ Circular • Gas : H_2	• B_T : 2 ~ 3.5 T • I_P > 0.3 MA • t_P > 2 s • Te ~ 1 keV • Shape ~ Circular • Gas : D_2	• B_T : 2 ~ 3.5 T • I_P > 0.5 MA • t_P > 5 s • Ti ~ 1 keV • Shape ~ DN (κ2.0) • Gas : D_2	• B_T : 2 ~ 3.5 T • I_P > 1 MA • t_P > 10 s • Ti ~ 3 keV • Shape ~ DN & SN • Gas : D_2	• B_T : 2 ~ 3.5 T • I_P > 1 MA • t_P ~ 20 s • Ti ~ 5 keV • Shape ~ DN & SN • Gas : D_2
Magnetic Control	• TF : 15 kA [1.5T) • PF : 4 kA (~1 Wb) • Grid : 50 MVA	• TF : 35 kA [3.5 T] • PF : +/-4 kA (~2 Wb) • Grid : 50 MVA	• TF : 35 kA [3.5 T] • PF : +/-10 kA (~4 Wb) • IVCC : VS • Grid: 100 MVA	• TF : 35 kA [3.5 T] • PF : +/-15 kA (~6Wb) • IVCC : VS • Grid: 100 MVA	• TF : 35 kA [3.5 T] • PF : +/-20 kA (~8Wb) • IVCC : FEC,RMP,RWM • Grid: 100 MVA
Vacuum Conditioning	• Inboard limiter (belt) • Gas puff • Glow DC	• Inboard limiter + Boronization + ICRF DC	+ Divertor + Passive stabilizer + In-vessel coil + PFC baking	+ PFC cooling	+ Cryopump operation
Heating & Current Drive	• ECH(84G):0.3MW, 0.4s	• ECH(110G): 0.2MW, 2s • ICRH: 0.3MW, 1s	• ECH(110G): 0.5MW • ICRH: 1MW • NBI: 1MW	• ECH(84/110G): 0.5MW • ECCD(170G): 1MW • ICRH : 1.5MW • NBI: 2MW • LHCD: 0.3MW	• ECH(84/110G): 0.5MW • ECCD(170G): 1MW • ICRH : 1.5MW • NBI : 5MW • LHCD : 0.3MW
Diagnostics	• Magnetic Diagnostics / MMWI / ECE / Hα / VS / filterscope / TV / • Hall probe array	+ XICS / Soft X-ray / Hard X-ray/ Resistive Bolometer / Probe / Reflectometer • e-beam	+ Thomson/ ECEI / IRTV / Image Bolometer / CES / neutron / XICS-2 / Ellipsometry /	+ FIR / Div. bolometer / X-ray pinhole / Coherence imaging/ fast-ion / etc	+ MSE / MIR / BES / VUV / CX-NPA /etc

References

[1] Y.K. Oh, et al., Fusion Eng. Des., **84** (2009) 344-350.
[2] E. Tsitrone, J. Nucl. Mater. **363-365** (2007) 12-23.
[3] S.H. Hong et al., Fus. Eng. Des. **85** (2010) in press.
[4] S.H. Hong et al., submitted to Nucl. Fusion.
[5] S.H. Park, et al., in this conference.
[6] Y.S.Park, S.A. Sabbagh, et al., in this conference.
[7] G.S. Lee, D.P. Ivanov, H.L. Yang, Hogun Jhang, J.Y. Kim, D.K. Lee, K.I. You, H.K. Kim, J.S. Bak, M. Kwon, J.H. Han, J. Last, ITC2001, Japan, 2001.
[8] Hogun Jhang, C.E. Kessel, N. Pomphrey, Jin-Yong Kim, S.C. Jardin, G.S. Lee, Fusion Eng. Des. **54** (2001) 117–134.
[9] D. Kim, H. Han, K.M. Kim, et al., Plasma Phys. Control. Fusion **52**(2010) 095009.
[10] H.K. Kim, H.L. Yang, et al., Fusion Eng. Des. **84** (2009) 1029-1032.
[11] S.H. Jeong, et al., Rev. Sci. Instrum. **79**, 02B310 (2008).
[12] Y.S. Bae et al., Nucl. Fusion **49** (2009) 022001.
[13] ITER DDD of "Lower Hybrid Heating and Current Drive System," G 54 DDD 201-07-19W 0.2.
[14] S. Park, H. Do, J.H. Jeong, W. Namkung, M.H. Cho, H. Park, Y.S. Bae, H.L. Yang, R. Ellis, J.R. Wilson, J. Hosea, Fusion Eng. Des. **85** (2010) 197-204.
[15] W.C. Kim, *et al*., in IAEA 2008 FEC, EX-C, PD/P1-2.
[16] S.W. Yoon, *et al*., in this conference.
[17] A.C. England, S.W. Yoon, W.C. Kim, et al., Fusion Eng. Des. (2010), doj:10.1016/j.fusengdes.2010.07.021.
[18] Y.M. Jeon. *et al*., in this conference.
[19] Portonea, et al., Fusion Eng. Des. **83** (2008) 1619.
[20] J. Winter, Plasma Phys. Controlled Fusion, **38** (1996) 1503-1542.
[21] D. Douai, T. Wauters, S. Bremond, E. de la Cal, G. Lombard, A. Lyssoivan, B. Pergourie, E. Tsitrone, and Tore Supra Team, Special Expert Working Group on Fuel Removal, 16. June. 2009.
[22] Private communication, 12th ITPA Div/SOL group meeting report.
[23] G. Federici, et al., External Report PPPL-3512, IPP-9/128, January, 2001.
[24] S. Hong, 2004, *PhD Thesis,* Ruhr-University Bochum, Bochum, Germany.
[25] Suk-Ho Hong, A. Murari, T. Loarer, A. Huber, C. Grisolia, P. Monier-Garbet, J. Winter and JET EFDA contributors, EFDA–JET–PR(09)24.
[26] Jae-Chun Seol, C.C. Hegna and J.D. Callen, Phys. Plasmas **16**, 052512 (2009).
[27] Jae-Chun Seol, B.H. Park, S.S. Kim, J.Y. Kim and Yong-Su Na, Nucl. Fusion **50**, 105008(2010).
[28] B.H. Park et al., submitted to Phys. Plasmas.
[29] C. B. Forest, Y. S. Hwang, M. Ono, and D. S Darrow, Phys. Rev. Lett. **68**, 3559 (1992).
[30] S. S. Kim, S. W. Yoon and J. Y. Kim, Journal of Kor. Phys. Soc. **56**, 1119 (2010).
[31] Sumin Yi, J.Y. Kim and C.M. Ryu, Fusion Eng. Des. **85**, 796 (2010).
[32] Y.S. Na, et al., Nucl. Fusion, **49** (2009) 115018.